

Pulsed single-photon spectrograph by frequency-to-time mapping using chirped fiber Bragg gratings

Alex O. C. Davis,¹ Paul M. Saulnier,¹ Michał Karpiński,^{1,2,*} and Brian J. Smith^{1,3}

¹*Clarendon Laboratory, University of Oxford, Parks Road, Oxford, OX1 3PU, UK*

²*Faculty of Physics, University of Warsaw, Pasteura 5, 02-093 Warszawa, Poland*

³*Department of Physics and Oregon Center for Optical, Molecular, and Quantum Science, University of Oregon, Eugene, Oregon 97403, USA*

A fiber-integrated spectrograph for single-photon pulses based upon frequency-to-time mapping, implemented by chromatic group delay dispersion (GDD), and precise temporally-resolved single photon counting is presented. A chirped fiber Bragg grating provides low-loss GDD mapping the frequency distribution of an input pulse onto the temporal envelope of the output pulse. Time-resolved detection with fast single-photon-counting modules enables the monitoring of the 825 nm to 835 nm wavelength range with nearly uniform efficiency with 55 pm resolution (24 GHz at 830 nm). To demonstrate the versatility of this technique spectral interference of heralded single photons and the joint spectral intensity distribution of a photon-pair source are measured. This approach to single-photon-level spectral measurements provides a route to realize applications of time-frequency quantum optics at visible and near-infrared wavelengths, where multiple spectral channels must be simultaneously monitored.

Optical experiments involve three essential steps, namely generation, manipulation and detection of light. Depending upon the demands of a specific application, different sources, modulation techniques and measurements are required. In the case of quantum optics, non-classical states of light enable performance beyond that possible with classical resources alone in a range of applications such as precision metrology [1, 2], and quantum key distribution [3]. Here information can be encoded in a variety of degrees of freedom, such as the amplitude and phase of a single field mode [4], the polarization [5], or the transverse-spatial mode [6] of a single photon. Pulsed wave-packet modes of light, in which the arrival time and central frequency of a pulse can be used as robust information carriers, are ubiquitous in classical telecommunications due to their natural compatibility with integrated-optical platforms and unprecedented information capacity. These pulse modes have recently gained significant interest in quantum optics both for quantum information processing applications [7] and metrology [8]. To harness the advances enabled by single-photon spectral mode encoding requires the ability to monitor many frequency channels concurrently arising from the fact that the information content in a given measurement is determined by the number of distinct measurement outcomes possible.

In this Letter, a method to simultaneously monitor multiple spectral channels of a pulsed single-photon source is proposed and demonstrated. Our approach utilizes the dispersive Fourier transform concept [9–11] to map the frequency of a temporally-short optical pulse onto the temporal envelope of the output pulse. We use advances in chirped fiber Bragg grating (CFBG) technology [12, 13] to achieve large linear group-delay dispersion (GDD) across a broad spectral range outside the telecommunications spectral region. At the output of the CFBG the time of arrival at a single fast single-photon counting module (SPCM) enables concurrent monitoring of multiple spectral modes in a single-photon wave packet. This technique allows high-resolution spectral measurement across

a broad frequency range with dramatic reductions in measurement time. The concurrent monitoring of many frequency modes enables multiple bits of information to be encoded per single photon. To demonstrate the wide-ranging applicability of this method we present spectral measurement of a heralded single-photon source occupying a double pulse mode that displays spectral interference fringes with unprecedented resolution and the joint spectral intensity from a degenerate two-photon source.

Two general approaches can be taken to acquire the spectrum of a beam of light. One approach involves scanning an optical element that maps spectral information onto the amplitude of the beam followed by direct intensity detection. This forms the basis of spectral measurements using Fabry-Perot etalons and Fourier-transform spectrometers. The alternative approach couples spectral modes with another set of modes such as transverse spatial modes. This technique underlies the standard spectrograph in which an angular dispersion element, such as a prism or grating, maps the spectral modes of an input optical beam onto a range of transverse spatial frequencies that can be transformed into localized points by a lens and monitored with an array of intensity detectors. Each approach has different advantages, for example methods that involve scanning require only a single detector and achieve high spectral resolution. However, scanning methods suffer from the time needed to acquire full spectral information and can be limited in the overall spectral range that can be readily accessed. The spectra of heralded single-photon and two-photon states have been realized using scanning monochromators [14] and Michelson interferometers [15]. A significant drawback to such scanning measurements is that they do not allow access to all spectral modes simultaneously, reducing the information content available in a single measurement outcome, and thus they cannot be used for real-time information processing or communications. This is incompatible with quantum applications that rely on the increased channel capacity offered by TF encoding.

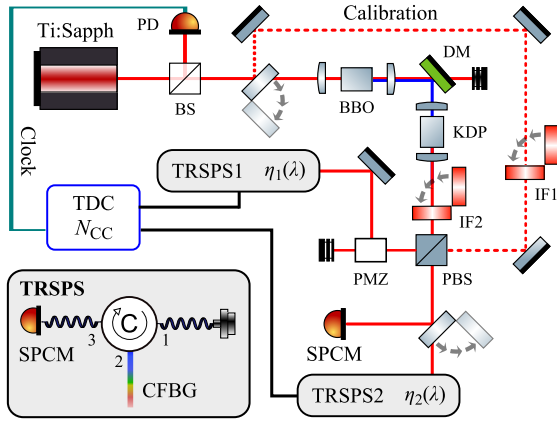


FIG. 1: Experimental setup. Ti:Sapph, Ti:sapphire femtosecond oscillator; BBO, beta barium borate & KDP, potassium dihydrogen phosphate crystals; (P)BS, (polarizing) beamsplitter; PD, fast photodiode; TDC, time-to-digital converter; DM, dichroic mirror; IF1(2), bandpass filters; PMZ, polarization Mach-Zehnder interferometer; TRSPS1(2), time-resolved single photon spectrograph; SPCM, single photon counting module. For calibration the TRSPSs were fitted with linear PDs. See text for details of the experiment.

In principle, mapping frequency modes of a beam onto the transverse spatial modes allows simultaneous monitoring of all spectral channels with a spatial array of detectors. However, this approach is difficult to realize at the single-photon level where coincidence events must be registered, owing to challenges in fabrication of large, low-noise and highly efficient arrays of independent single-photon-counting detectors [16]. The frequency distribution of pulsed light can be mapped onto temporal modes by a medium with high GDD and monitored with a single intensity detector with high temporal resolution [9, 11]. At the single-photon level this method was used to construct a single-photon spectrograph at telecommunications wavelengths [17] where a 3.3 km long dispersion compensating fiber introduced the necessary GDD. Within the visible spectral domain significant losses in optical fibers make this approach infeasible. This challenge can be overcome by using low-loss chirped fiber Bragg gratings (CFBGs) as the dispersive medium [18, 19]. Here we combine this technique with time-resolved single photon detection presenting a high-resolution single photon spectrometer that allows simultaneous monitoring of multiple spectral modes using a single detector at high repetition rates.

The time-resolved single-photon spectrometer (TRSPS) is constructed from a fiber-based optical circulator (FCIR-2285-14B181, Haphit) spliced to a chirped fiber Bragg grating (CFBG, TeraXion) operating in reflection, with the circulator output directed to a fast SPCM as depicted in Fig. 1 (inset). The pulse to be characterized is launched into port 1 of the circulator and directed to port 2, where it is reflected by the CFBG, which provides constant GDD. The reflected pulse emerges from port 3 of the circulator and is detected by a fast SPCM (PDM, Micro Photon Devices) with approximately 55 ps timing jitter. The SPCM signal is monitored

by a time-to-digital converter (TDC, PicoQuant, HydraHarp 400) triggered by a fast photodiode signal that samples the laser pulse train acting as the experiment clock. The TDC has timing resolution down to 1 ps, below the detector timing resolution and the trigger photodiode (Alphas, UPD-15-IR2-FC) has approximately 15 ps rise time and timing resolution less than 1 ps. The TDC records a list of times between trigger events and SPCM signals, $\{\tau_j\}$, which are then converted into a histogram of coincidence counts as a function of these times, $N_{CC}(\tau)$. The time bin size of 32 ps is chosen to be smaller than the SPCM timing jitter.

The wavelength-dependent time of arrival relative to a pulse centred on the centre wavelength of the CFBG ($\lambda_0 = 830$ nm) is $t = D(\lambda - \lambda_0)$, where D is the GDD of the CFBG. Thus the spectral intensity of heralded single photons, $S(\lambda)$, from this histogram will be

$$S(\lambda) = N_{CC}(D\lambda - \delta\tau)/\eta(\lambda), \quad (1)$$

where $\eta(\lambda)$ is the wavelength-dependent efficiency of the TRSPS, including contributions from both the circulator-CFBG setup and the efficiency of the SPCM. The time offset $\delta\tau$ depends upon optical and electronic delays in the experiment and sets the central wavelength of the distribution. Thus, to determine the spectrum of pulsed single photons, the time $\delta\tau$, GDD D , and efficiency $\eta(\lambda)$ must be ascertained.

The temporal point-spread function of the detector-TDC setup has a full-width at half-maximum (FWHM) width 55 ps. This was determined by sending single photons directly into the setup, bypassing the CFBG, and measuring the resulting temporal distribution. The CFBG introduces approximately 950 ps/nm of GDD to the optical pulse train centered about 830 nm wavelength, resulting in a frequency-dependent group delay that allows direct measurement of the pulse spectrum with time-resolved detection. The spectral resolution is set by the ratio of detector timing resolution, Δt and GDD $\Delta\lambda = \Delta t/D = 0.05$ nm. The CFBG reflectivity $R \approx 0.5 \pm 0.05$ is nearly constant across a wavelength range of 825 – 835 nm. The total optical transmission through the device was measured by launching broadband classical pulses into the spliced circulator-CFBG combination and monitoring the input and output spectral intensity with a standard spectrometer (Andor Shamrock 303i monochromator, 1200 mm grating, combined with Andor iDus CCD camera) with 0.054 nm resolution. This is approximately 0.1 across the 825-835 nm wavelength range, and includes losses in the circulator and fiber splices. All these sources of loss are technical in nature and could be reduced with further development.

To determine D , laser pulses with narrow bandwidth derived from a spectrally-filtered Ti:Sapphire oscillator were routed into the device. The pulse train was passed through a 1 nm bandwidth interference filter (Andover Corp., USA) (IF2 in Fig. 1, which was tilted such that the narrowband transmitted light could be tuned across the range 825-835 nm. Its spectrum was measured with the conventional spectrometer. The output of the circulator was coupled into a fast photodiode (DET10C, Thorlabs) and the delay of the signal relative

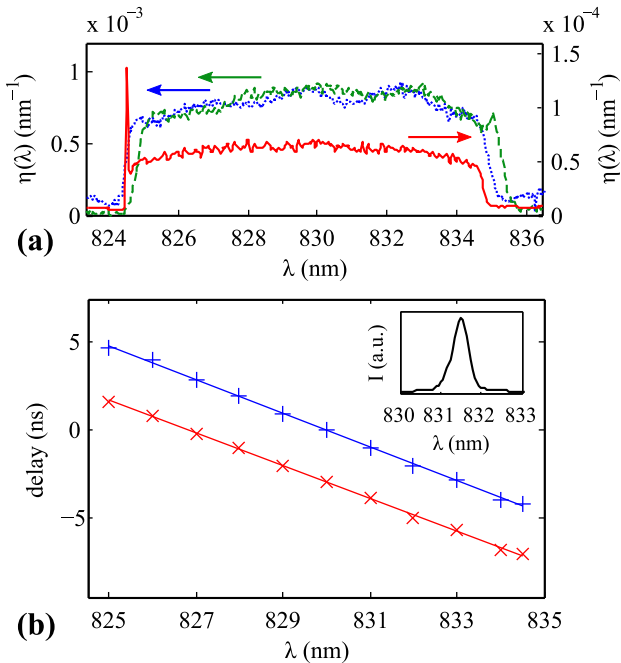


FIG. 2: (a) Spectral response functions of the three TRSPS setups. Data normalized to their integral equaling total heralding efficiency, such that $\eta(\lambda)$ corresponds to the probability density of detecting a photon at λ given a uniform prior, conditional on a heralding event. Response is close to zero outside of the 825 – 835 nm reflection window of the CFBGs. CFBG1 (dotted, blue) and CFBG2 (dashed, green) with Perkin-Elmer (slow) SPCMs. CFBG1 with MPD (fast, less efficient) SPCM (solid red, right scale). The peak at 824.6 nm is caused by back-reflection from a fibre splice. This feature is present in the dotted dataset as well but is not resolved by the slower SPCM. (b) Wavelength-dependent delays introduced by the CFBGs, obtained using bright laser pulses for spectrometers 1 (black) and 2 (red) with linear fits (solid lines). INSET: Example of narrowband filtered spectrum used for calibration.

to the experiment clock (driven by the laser pulse train) was measured on an oscilloscope (Tektronix MSO 5104). The measured delay as a function of wavelength is presented in Fig. 2(b) for two different circulator-CFBG setups. A polynomial fit applied to the data yields a GDD of 938 ps/nm and 958 ps/nm in TRSPS 1 and 2 respectively. Higher-order wavelength dependence of the time delay was negligible and is henceforth neglected. The value of $\delta\tau$ depends on electronic and optical delays and so needs to be determined independently for each experimental setup. For the calibration setup (shown by the dotted line in Fig. 1, the spectrally filtered bright pulses were set to 830 nm center wavelength and the CFBG-circulator setup attached to a fast SPCM and TDC to complete the TRSPS. The peak in the temporal histogram can then be associated with the center wavelength of the calibration pulse, and with D known, all the single-photon time tags τ_i can be attributed to specific wavelength values. In the subsequent demonstrations involving single photons, where the beam follows a different path (the downconversion path shown by the solid line in Fig. 1), the timing offset $\delta\tau$ is re-

covered in the same fashion by using narrowband filtration of the single-photon light source itself with filter IF1 and comparing with the known spectrum transmitted by the filter, obtained with a long integration time measurement on the standard spectrometer.

To determine the efficiency $\eta(\lambda)$, the same beam path – the dotted line in Fig. 1 – is used without the filter IF2. Removing this filter subtracts only about 6 ps of delay, less than the temporal resolution of the SPCM, and therefore to within the resolution of the device the same value for $\delta\tau$ is retained. The spectral intensity, $I_{\text{in}}(\lambda)$, of an attenuated classical pulse is measured with the conventional spectrometer at the output of the laser. This pulse is then directed through the TRSPS setup and the total singles count rate at the output, $N_S(\lambda)$, is measured, enabling characterization of the wavelength dependent response $\eta(\lambda) = N_S(\lambda)/AI_{\text{in}}(\lambda)$, where A is a normalization chosen such that $\int \eta(\lambda)d\lambda = H$, where H is the total heralding efficiency of the setup. The resulting response function $\eta(\lambda)$ for the three TRSPS setups used is shown in Fig. 2(a).

To demonstrate the versatility of this device, we first measure the spectrum of heralded single photons occupying a double pulse displaying spectral interference fringes. Heralded single photons are generated by collinear, type-II spontaneous parametric down conversion (SPDC) in an 8 mm long potassium di-hydrogen phosphate (KDP) crystal [14]. The KDP crystal is pumped by a frequency-doubled Ti:Sapphire laser oscillator in 0.7 mm thick beta barium borate (BBO) operating at 80 MHz repetition rate with 830 nm central wavelength and 7 nm bandwidth. The orthogonally polarized degenerate signal and idler fields with 2 nm and 8 nm FWHM bandwidths, respectively, are separated at a polarizing beam splitter (PBS), with a photodetection event in the broadband idler mode heralding the existence of a photon in the narrowband signal mode. To produce a single photon in a double pulse, the heralded photon of 2 nm bandwidth is sent through a half wave plate (HWP) rotating the polarization to 45° followed by a Soleil-Babinet compensator (SBC) that introduces a controllable group delay, T , between horizontal (H) and vertical (V) polarization modes. The time delay T was determined from the fringe spacing in the interference pattern of classical light sent through the interferometer. An additional HWP rotates the H (V) polarization to (anti-)diagonal polarization and a polarizer selects H polarized components of the field to be transmitted, probabilistically yielding a single-photon double pulse. The double pulse train output was sent to the TRSPS to analyze the spectrum. The spectrum of the heralded double pulse is obtained by using the heralding detection event to trigger the TDC and the detection time of the signal photon. The resulting spectral interference pattern, shown in Fig. 3(a), displays an oscillation period of approximately 0.2 nm, well matched to the time delay $T = 11$ ps introduced by the SBC. This spectrum, acquired over 600 s, contains 28000 heralded single photon detection events.

To further demonstrate the utility of the TRSPS, the joint spectral intensity (JSI) of the SPDC source was measured. This was achieved by directing the idler photon to a second

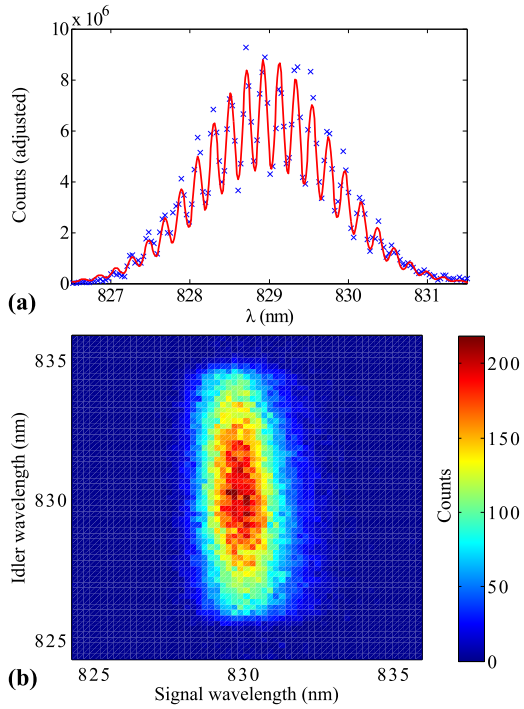


FIG. 3: (a) Experimental heralded single photon spectrum in a double-pulse mode. The spectrum has been processed to account for the variation in efficiency $\eta(\lambda)$ across the wavelength range. The red curve shows the expected spectrum given the underlying single photon spectrum and the time delay, with visibility and phase chosen freely in order to give the best fit. To obtain the red curve, a Gaussian fit to the underlying spectrum was obtained from a separate measurement of the photon spectrum; this was modulated by a sinusoidal signal with known period given by the time delay. (b) Measured JSI of SPDC photon pair source. Coincidence counts per bin, adjusted to account for the spectral variation of TRSPS efficiency.

TRSPS, sending the signal photon directly into the TRSPS and observing coincidence events between the signal and idler modes. Previously, the JSI in the stimulated emission regime has been characterized using a bright continuous wave seed in the idler mode to create a bright signal beam that can be resolved conventionally, enabling high spectral resolution and S/N ratio compared to scanning monochromators [20]. However, directly resolving individual photon pairs in the spontaneous emission regime has been achieved away from telecommunications wavelengths using variants on scanning methods in which most photons are discarded [14, 21] or the spectral bins were not monitored directly [22]. The approach described here allows simultaneous monitoring of many spectral modes and therefore far higher count rates and shorter acquisition times and communications. The recently proposed spectral-spatial-temporal mapping setup [23] is conceptually similar to our method, albeit lacks the all-fiber character and achieves much lower resolution over a limited spectral range.

To enable sufficient coincidence count rates, for the joint measurement more efficient SPCMs were employed (Perkin Elmer SPCM-AQ4C). These detectors have quantum effi-

ciency of approximately 0.4 at 830 nm central wavelength, which comes at the cost of reduced timing resolution, $\Delta T = 200$ ps, and thus lower spectral resolution $\Delta\lambda = 0.2$ nm, that can be achieved. The coincidence timing was implemented using a lower-timing-resolution TDC (quTAU, quTOOLS; 81 ps timing resolution), capable of a higher number of input channels than the fast TDC, which allowed us to easily monitor two TRSPS triggered by the clock signal derived from the Ti:Sapphire pulse train. To extract the JSI for the SPDC source each TRSPS was calibrated in turn in the same manner as for the heralded single photon interferogram experiment, and then time stamps at each SPCM are used to determine the corresponding wavelengths. The normalized JSI is shown in Fig. 3(b). Note that full spectrum of the idler photon is not accessible because the reflectivity of the CFBG is limited to a 10 nm range about 830 nm. This could be improved by exchanging the FBGs by those with broader spectral range.

In summary, we have demonstrated a method to provide high-resolution, simultaneous monitoring of the spectrum of pulsed modes at the few-photon level. The approach utilizes frequency-to-time mapping introduced by large second-order dispersion in a chirped fiber Bragg grating followed by fast time-resolved detection. The calibration of the device can be achieved using a narrowband classical light source and conventional spectrometer. This approach enables conditional high resolution spectral measurement of light allowing acquisition rates that are orders of magnitude faster than previously achieved. We anticipate this method will find use in a broad range of applications for low light sensing from quantum foundations to technologies such as time-frequency quantum key distribution.

Funding

This project has received funding from the European Community (EC) Horizon 2020 research and innovation programme under Grant Agreement No. 665148 and the United Kingdom Defense Science and Technology Laboratory under contract No. DSTLX-100092545. MK was partially supported by the PhoQuS@UW project (Grant Agreement No. 316244) within the EC 7th Framework Programme, as well as by the National Science Centre of Poland project No. 2014/15/D/ST2/02385.

Acknowledgements

We thank E. Poem and M. Nejbauer for insightful discussions and D. Gauthier for assistance in acquiring the CFBGs.

* Electronic address: mkarp@fuw.edu.pl

- [1] J. Aasi, J. Abadie, B. P. Abbott, R. Abbott, T. D. Abbott, M. R. Abernathy, C. Adams, T. Adams, P. Addesso, R. Adhikari *et al.*, Nat. Photon. **7**, 613 (2013).
- [2] R. Demkowicz-Dobrzański, J. Kołodyński, and M. Guță, Nat. Commun. **3**, 1063 (2012).
- [3] J. Nunn, L. J. Wright, C. Söller, L. Zhang, I. A. Walmsley, and B. J. Smith, Opt. Express **21**, 15959 (2013).
- [4] P. C. Humphreys, W. S. Kolthammer, J. Nunn, M. Barbieri, A. Datta, and I. A. Walmsley, Phys. Rev. Lett. **113**, 130502 (2014).
- [5] A. Poppe, A. Fedrizzi, R. Ursin, H. Böhm, T. Lörünser, O. Maurhardt, M. Peev, M. Suda, C. Kurtsiefer, H. Weinfurter *et al.*, Opt. Express **12**, 3865 (2004).
- [6] B. Jack, A. M. Yao, J. Leach, J. Romero, S. Franke-Arnold, D. G. Ireland, S. M. Barnett, and M. J. Padgett, Phys. Rev. A **81**, 043844 (2010).
- [7] B. Brecht, D. V. Reddy, C. Silberhorn, and M. G. Raymer, Phys. Rev. X **5**, 041017 (2015).
- [8] B. Lamine, C. Fabre, and N. Treps, Phys. Rev. Lett. **101**, 123601 (2008).
- [9] Y. C. Tong, L. Y. Chan, and H. K. Tsang, Electron. Lett. **33**, 983 (1997).
- [10] V. Torres-Company, J. Lancis, and P. Andrés, Prog. Opt. **56**, 1 (2011).
- [11] K. Goda and B. Jalali, Nat. Photon. **7**, 102 (2013).
- [12] J. Canning, Laser Photon. Rev. **2**, 275 (2008).
- [13] M. Ibsen, M. Durkin, M. Zervas, A. Grudinin, and R. Laming, IEEE Photonic Tech. Lett. **12**, 498 (2000).
- [14] P. J. Mosley, J. S. Lundeen, B. J. Smith, P. Wasylczyk, A. B. U'Ren, C. Silberhorn, and I. A. Walmsley, Phys. Rev. Lett. **100**, 133601 (2008).
- [15] W. T. Buttler, R. J. Hughes, P. G. Kwiat, S. K. Lamoreaux, G. G. Luther, G. L. Morgan, J. E. Nordholt, C. G. Peterson, and C. M. Simmons, Phys. Rev. Lett. **81**, 3283 (1998).
- [16] F. Zappa, S. Tisa, A. Tosi, and S. Cova, Sensor. Actuat. A: Phys. **140**, 103 (2007).
- [17] M. Avenhaus, A. Eckstein, P. J. Mosley, and C. Silberhorn, Opt. Lett. **34**, 2873 (2009).
- [18] M. A. Muriel, J. Azaña, and A. Carballar, Opt. Lett. **24**, 1 (1999).
- [19] J. Azaña and M. A. Muriel, IEEE J. Quant. Electron. **36**, 517 (2000).
- [20] B. Fang, O. Cohen, M. Liscidini, J. E. Sipe, and V. O. Lorenz, Optica **1**, 281 (2014).
- [21] Y.-H. Kim and W. P. Grice, Opt. Lett. **30**, 908 (2005).
- [22] W. Wasilewski, P. Wasylczyk, P. Kolenderski, K. Banaszek, and C. Radzewicz, Opt. Lett. **31**, 1130 (2006).
- [23] E. Poem, T. Hiemstra, A. Eckstein, X.-M. Jin, and I. A. Walmsley, Opt. Lett. **41**, 4328 (2016).